Biomacromol. J., Vol. 5, No. 2, 105-112, December 2019.

Biomacromolecular Journal
www.bmmj.org

A Nanocarrier Based on Protein and Reduced Graphene Oxide for Sustained Release and Improvement of Carboplatin Efficacy in Cancer Treatment

J. Khodadi[a], M. Saeidifar[a,*], M. Shahlaei[a], A. Divsalar[b] and P. Sangpour[a]

[a]*Department of Nanotechnology and Advanced Materials, Materials and Energy Research Center, Karaj, Iran*

[b]*Department of Biological Sciences, Kharazmi University, Tehran, Iran*

(Received 29 March 2020, Accepted 14 June 2020)

ABSTRACT

Nano-drug delivery has attracted great attention in improving the efficacy of anticancer drugs. This study described the preparation of a nanosize carrier based on protein and reduced graphene oxide (rGO) for sustained release and the enhancement of the treatment efficacy of carboplatin in breast cancer cell lines. Moreover, the characterization of bovine serum albumin nanoparticles (BSANP)-coated rGO nanosheets (rGO-BSANP) was performed by FTIR, DLS and SEM techniques. The results demonstrated that BSANP and rGO bond to each other with an average size of 753.1 nm and a surface charge of -16.0 mV. Entrapment efficiency and drug loading of rGO-BSANP in three different ratios (1:1, 1:5 and 1:10) were determined. *In vitro* carboplatin release from rGO, BSANP and different ratios of rGO-BSANP at 300 min showed that the rGO-BSANP nanocarrier with 1:1 ratio was an appropriate system. Furthermore, the cytotoxicity of carboplatin, rGO-BSANP and carboplatin loaded rGO-BSANP (car@rGO-BSANP) was evaluated using the MTT assay, on breast cancer cell lines, MCF7. Results showed that the presence of nanocarrier caused IC_{50} of carboplatin significantly decreased. Hence, the designed nanocarrier helps sustained release and a lower concentration of carboplatin for cancer treatment.

Keywords: BSA nanoparticle, rGO, Release, Carboplatin, Mechanism

INTRODUCTION

Carriers based on hydrogel and particles have been studied most recently for sustained and prolonged drug supply [1-3]. Several drug nano-vehicles have been studied in cancer treatment to reduce side effects and improve therapeutic efficacy because chemotherapeutic drugs not only can destroy cancer cells but also, damage the healthy cells [3,4]. Therefore, drug delivery systems can be used for prolong release and maintaining the drug dose in the therapeutic window and decreasing side effect [5,6]. Among the drugs most commonly used are derivatives of Pt(II) complexes like cisplatin or carboplatin. Carboplatin is a treatment for many different types of cancer such as ovarian cancer, lung cancer, and brain cancer and has fewer side effects than other platinum-based drugs such as cisplatin [7]. However, carboplatin has poor cellular uptake and require high dose administration in multiple cycles to achieve tumor inhibition, due to these features, encapsulation and sustained release of drug can be reducing the side effects and improving its therapeutic potential. Sadhukha and Prabha concluded despite of hydrophilic nature, carboplatin was loaded into PLGA nanoparticle and encapsulating carboplatin improves anti-cancer efficiency [8]. Liposomal platinum(II) formulation is a way to improve therapeutic potential that shows highlighted to passively accumulate at tumor sites with enhanced permeability and retention effect (EPR) in inflamed abnormal capillaries and lymphatic system [9-11]. Another strategy is using protein carriers such as bovine serum albumin (BSA); due to biodegradable, biocompatible, non-immunogenic, and nontoxic feature. BSA can be bind with other multiple ligands and it evolved to be a general transporter protein [12-14]. In the other hand, reduced graphene oxide (rGO) has used in many biomedical applications, including drug and gene delivery, tissue engineering, and biosensing and it is very reliable for photothermal therapy [15].

This study focused on the preparation and characterization of rGO-BSANP for the sustained release of carboplatin. After that, entrapment efficiency and

*Corresponding author. E-mail: saeidifar@merc.ac.ir

loading of carboplatin onto rGO, BSANP, and different ratios of rGO-BSANP (1:1, 1:5, 1:10) were studied. Furthermore, the release of carboplatin from carriers and their mechanism were investigated. Finally, the cytotoxicity evaluation of samples was performed using MTT assay on breast cancer cell lines, MCF7. It was attempted to introduce the rGO-BSANP nanocarrier as a sustained release system with lower side effects and efficacy enhancement ability in cancer treatment.

MATERIALS AND METHODS

Materials and Cell Lines

Bovine serum albumin (BSA, lyophilized powder, 67000 Da), glutaraldehyde solution (25%) as a crosslinking agent, phosphate buffer saline (PBS), carboplatin and dialysis tube (12 kDa) were purchased from Sigma Aldrich (Germany). Breast cancer cell lines, MCF-7 obtained from Pasteur Institute of Iran. Ethanol was obtained from Merck (Germany). Reduced graphene oxide (rGO) nanosheets were prepared in our lab [16]. Milli-Q water was used for preparation of all aqueous solutions.

Methods

Fourier transform infrared (FTIR) spectra were recorded by the Bruker Company of the Netherlands in the range of 4000-400 cm^{-1}. Scanning electron microscopy (SEM) images were taken by TESCAN VEGA-II, USA. Zeta potential and Zeta sizer were recorded by Malvern Instrument, Worcestershire, UK. Ultrasonic sonoswiss, SW6H model and Hettich® Universal 320/320R centrifuge, Germany were used. Absorption spectroscopy was adopted to study the drug release behavior by T80 + UV-Vis Spectrophotometer, UK.

Preparation of BSANP and rGO-BSANP

BSANP was prepared by desolvation method [17]. Briefly, 50 mg of bovine serum albumin was dissolved in 2 ml water with pH = 7.4, stirring (300 rpm) at room temperature. Afterward, 8 ml of ethanol was added with a rate of 0.5 ml min^{-1} stirring until the solution turned white; thus, the aggregation of protein chains was occurred. Then, 12 µl of glutaraldehyde (8%) was added to the above solution, cross-linking the process for 24 h [14,18-20]. Later, BSANP was purified by three cycles of centrifugation (11000 rpm for 10 min) at room temperature and redispersion of the pellet in 2 ml Milli-Q water.

For the rGO-BSA nanosheet synthesis, 50 mg rGO was suspended in 200 µl Milli-Q water and was added to 50 mg of aggregated BSA according to the above procedure. After 10 min, 12 µl of glutaraldehyde (8%) was added to the suspension and stirred at 300 rpm for 24 h. Next, the rGO-BSA nanosheet (rGO-BSANP 1:1 w/w) was purified by three cycles of centrifugation (11000 rpm for 10 min) at room temperature and redispersed in 2 ml Milli-Q water. This process was repeated for two different ratios of rGO to BSA, 1:5 w/w (50 mg of rGO and 250 mg of BSA) and 1:10 w/w (50 mg of rGO and 500 mg of BSA), respectively.

Drug Loading and Release Experiments

Drug loading. Loading carboplatin (3.59 mg) on BSANP (car@BSANP), rGO (car@rGO) and different ratios of rGO-BSANP (car@rGO-BSANP) was separately performed by mixing them (1:1 of drug/carrier) in PBS buffer (2 ml) under the stirring condition (400 rpm) for 24 h. Then, the solution was purified by one cycle of centrifugation (11000 rpm for 10 min) for the supernatant elimination at room temperature and redispersed in water. The supernatant was examined by UV-Vis at 230 nm (wavelength index) to realize the concentration of unloaded carboplatin according to the obtained equation from the standard plot.

Standard Equation

Different concentrations of carboplatin (0-0.07 mM) were prepared and their absorption was recorded at 230 nm. Then, the plot of absorption versus concentration was drawn and the best linear equation was calculated.

Entrapping and Loading Percentage of Drug

The encapsulation efficiency (%EE) and drug loading (%DL) were determined by following equations [21]:

$$\%EE = (M_0/M_1) \times 100 \quad (1)$$

$$\%DL = (M_0/M) \times 100 \quad (2)$$

Where M_0, M_1 and M were loaded carboplatin

concentration, total concentration of carboplatin and concentration of carrier, respectively.

Drug Release

Drug release from carriers was performed by the dialysis membrane (DM) method. For this purpose, the carrier was introduced into a dialysis bag (12 kDa) containing 15 ml of release media (PBS buffer) [22]. The immersion condition was maintained by periodically picking up a 3 ml sample and replacing an equal volume of buffer, and the amount of drug release was analyzed with UV-Vis at 230 nm. The cumulative drug release percentage was determined by following equation [23]:

$$\%\text{Cumulative release} = M/M_0 \times 100 \quad (3)$$

Where M is the concentration of released carboplatin from the carriers at time t and M_0 is total concentration of loaded carboplatin.

Release Mechanism

Evaluation of Carboplatin release mechanism was performed using three mathematical models as follow [24]:

-Zero-order model

$$M_t = M_0 + k_0 t \quad (4)$$

In above equation, M_t, M_0 are the amount of dissolvation drug in time t and the initial drug content, respectively. k_0 is the zero-order release constant. The zero-order kinetic model is independent of drug concentration and an ideal pattern for poorly soluble drug or slow drug delivery (such as anticancer and antibiotic drugs), transdermal, and ophthalmic.

-First-order model

$$\log M_t/M_0 = -k\, t/2.303 \quad (5)$$

M_t, M_0 and t are the same of Zero-order model, and k is the first-order release constant. The first-order kinetic model is independent of drug concentration.

-Korsmeyer-Peppas model

$$\log M_t/M_\infty = \log k_p + n\log t \quad (6)$$

Where M_t/M_∞ is the fraction of drug release at time t, n is the release index and value to predict the mechanism of release ($n < 0.43$ was Fickian diffusion and n between 0.43-1 was non-Fickian diffusion in the drug release process) and k_p is the Korsmeyer-Peppas release rate constant [24]. In this model, 60% of the initial data were used for plotting diagrams.

The high determination coefficient (R^2) of each model showed the best-fit release model.

In Vitro Cytotoxicity Study

Cell viability percentage of car, rGO-BSANP (1:1 w/w) and car@rGO-BSANP (1:1 w/w) was evaluated on human breast cancer cell lines, MCF-7 by MTT (3-(4,5-dimethylthiazol-2-yl)-2-5-diphenyltetrazolium bromide) assay. The MCF-7 cells were seeded into 24-well culture plates at a density of 1×10^4 and cultured in DMEM supplemented with fetal bovine serum (FBS) at 37 °C with 5% CO_2. Then, various concentrations of carboplatin (0-1.4 mg ml) were added to the cell culture medium. The culture medium was used as blank control. MTT solution (5 mg ml^{-1}) was added to each well, and the cells were incubated for another 4 h, NADH reacted with a tetrazolium salt produced formazan with purple color. Then, the purple crystals of formazan were dissolved by adding DMSO, and the product was measured at 570 nm [25,26].

Cell Viability Analysis

The One-way ANOVA was applied to analyze the data of Cell viability. Multiple comparisons was carried out with a $p < 0.05$ statistical significance.

RESULTS AND DISCUSSION

Characterization

The FTIR spectra of rGO, BSANP, and rGO-BSANP with ratios of 1:5 and 1:10 were illastrated in Fig. 1a. In the spectrum of rGO, the bands in 1745 cm^{-1} and 1630 cm^{-1} were related to C=O, and 1400 cm^{-1} assigned to C=C graphene sheets. The BSANP spectrum showed the C-H

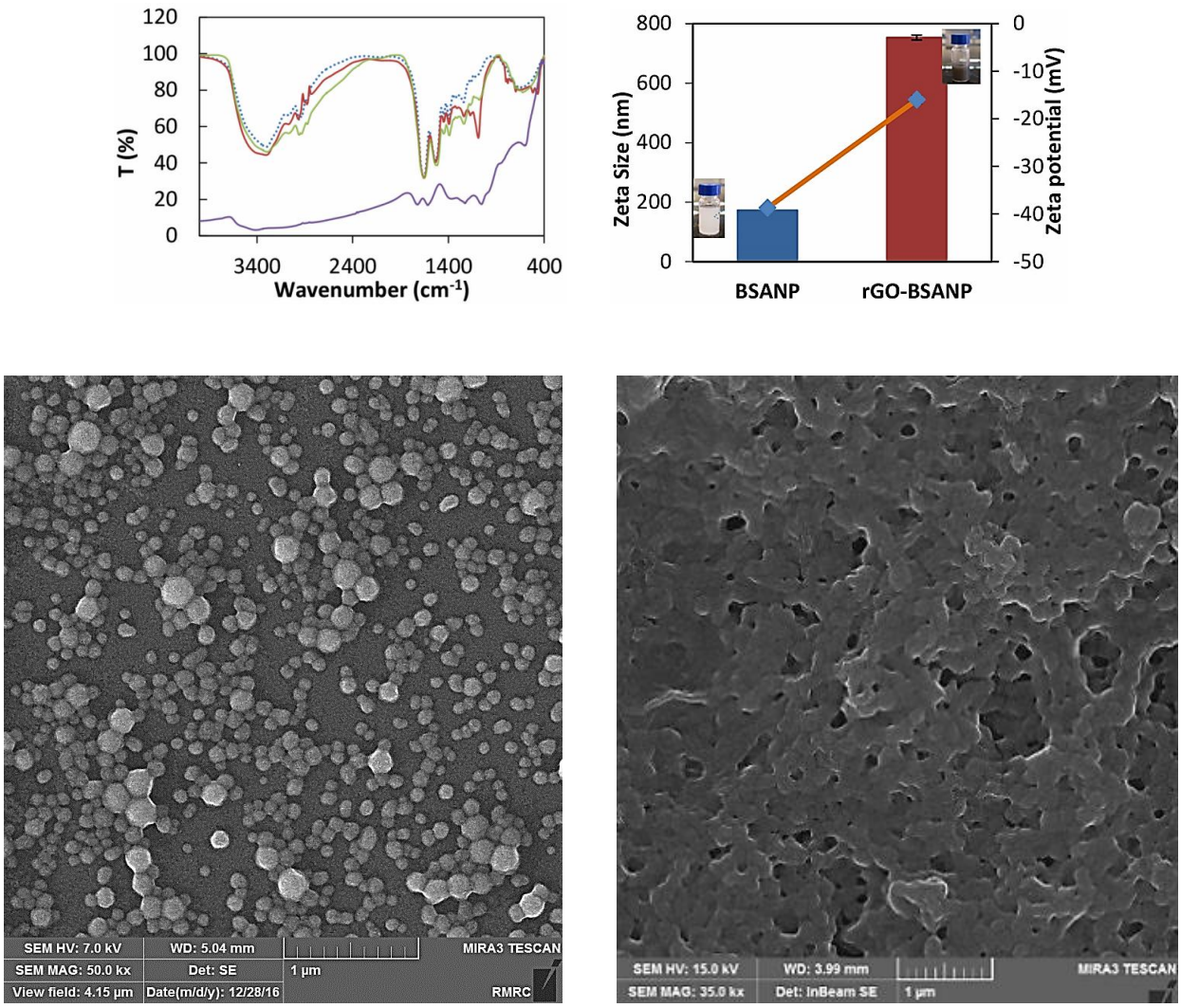

Fig. 1. FTIR spectra of rGO (yellow line), BSANP (blue dots), and rGO-BSANP (red and gray line with different proportions (1:5; 1:10)) (a); DLS of BSANP and rGO-BSANP (b) SEM images of BSANP (left), rGO-BSANP (1:10) (right) (c).

vibrations of methoxy group around 2952 cm^{-1} and 1665 cm^{-1} (amide I), related to the carbonyl group receiving a hydrogen bond from the amine group. There was a symmetrical stretching in 1400 cm^{-1} due to the COO^- group [27,28]. The rGO-BSANP spectrum demonstrated perfect protein coating on rGO just in 1089 cm^{-1} there is a small difference related to epoxy or C-OH in rGO [29].

Figure 1b shows the hydrodynamic diameter and zeta potential of BSANP and rGO-BSANP. The hydrodynamic size of rGO-BSANP (753.1 nm) was greater than BSANP (172.9 nm) due to the presence of rGO nanosheets. Furthermore, the surface charge of rGO-BSANP (-16.00 mv) was more positive than BSANP (-38.73), showing lower stability in the rGO-BSANP nanocarrier [30]. This phenomenon could be due to the repulsion between negative surface charges of rGO and BSANP.

SEM images of BSANP (Fig. 1c, left) showed a uniform size with a spherical shape and average particle size of

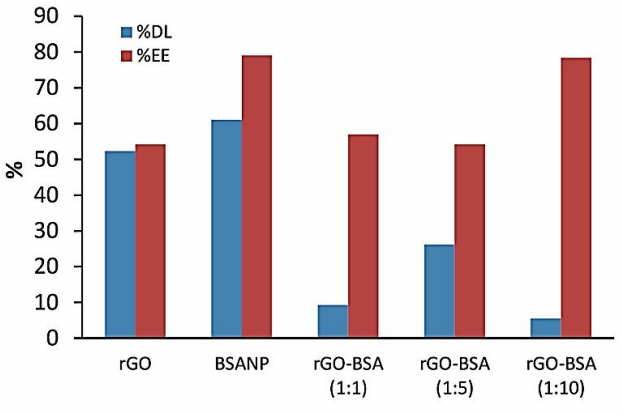

Fig. 2. Drug loading and encapsulation efficiency percentage of rGO, BSANP and rGO-BSANP (1:1; 1:5; 1:10).

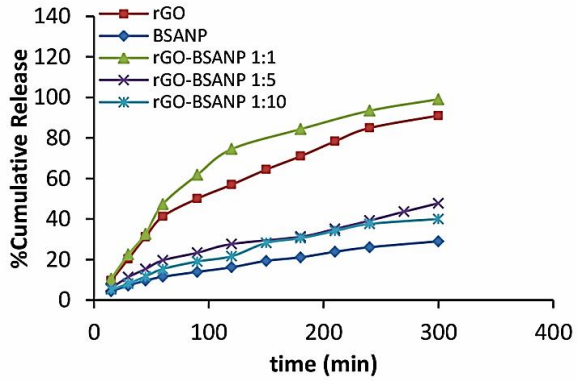

Fig. 3. *In vitro* carboplatin release curves from rGO, BSANP and rGO-BSANP (1:1; 1:5; 1:10) carriers.

170.17 nm. SEM images of rGO-BSANP indicated the edges of GO-NSs, a shown in Fig. 1c, right; they also showed that BSANP coated the surface of rGO sheets without any changes in the spherical shape and the average size of BSANP.

Encapsulation Efficiency and Drug Loading Study

Encapsulation efficiency (%EE) and drug loading capacity (%DL) were determined corresponding to Eqs. (1)-(2) and shown in Fig. 2. The carboplatin loading was significantly increased in rGO and BSANP relative to rGO-BSA, indicating that the interaction between rGO and BSANP reduced the binding sites for carboplatin. However, the encapsulation efficiency of all systems was approximately equal; thus, the maximum of the drug could be encapsulated.

Release Study

Carboplatin release profiles from rGO, BSANP, and rGO-BSANP (1:1, 1:5 and 1:10) were shown in Fig. 3. The cumulative release percentage for rGO and rGO-BSANP (1:1) systems was significantly greater than BSANP and rGO-BSANP (1:5 and 1:10) at 300 min, while %DL and %EE were almost equal together. This phenomenon may be due to the presence of rGO with a vast and accessible surface area for the release of drugs.

Release Mechanism

Zero-order, First-order, and Korsmeyer-Peppas mathematical models were utilized to analyze the *in vitro*

Table 1. Results of Kinetic Models

Sample	Zero order		First order		Korsmeyer-Peppas		
	$k_0 \times 10^{-3}$	R^2	$k \times 10^{-3}$	R^2	$k \times 10^{4}$	n	R^2
rGO	2.4	0.93	2.3	0.71	0.92	0.69	0.96
BSANP	2.5	0.98	2.9	0.87	5.87	0.62	0.99
rGO-BSANP (1:1)	2.8	0.87	2.7	0.07	0.98	0.74	0.97
rGO-BSANP (1:5)	1.2	0.94	2.8	0.77	2.29	0.63	0.97
rGO-BSANP (1:10)	3.9	0.98	3.4	0.87	7.39	0.71	0.99

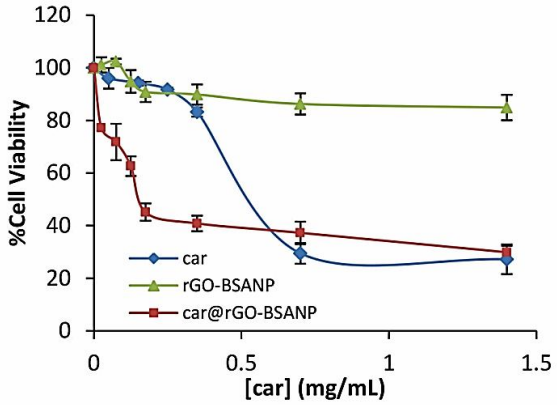

Fig. 4. Cell viability of MCF-7 onto car (0-1.4 mg ml^{-1}), rGO-BSANP (1:1), and car@rGO-BSANP (1:1).

released data and demonstrate its mechanism. Table 1 presents the correlation coefficients of three kinetic models. According to the summarized results, the release profile could be fit well with Korsmeyer-Peppas release kinetic model. Furthermore, the release of the systems was followed by non-Fickian diffusion since n value was between 0.43-1. Hence, the polymer relaxation time was approximately equal with the characteristic solvent diffusion time in the solute transport process in which the macroscopic drug release becomes anomalous or non-Fickian [31].

MTT Assay

As shown in Fig. 4, the rGO-BSANP carrier has no significant cytotoxicity thus the toxicity of rGO [32] is eliminated by biocompatible BSANP. In contrast, cell viability percentage upon adding carboplatin was decreased in the other two systems (car and car@rGO-BSANP). Therefore, cancer cell death was dose-dependent. Furthermore, the half maximal inhibitory concentration (IC_{50}) of car and car@rGO-BSANP was determined to be 0.52 mg ml^{-1} and 0.15 mg ml^{-1}, respectively. Consequently, the required dose to kill breast cancer cells in car@rGO-BSANP system was approximately 3.5 times lower than the car.

CONCLUSIONS

In this study, a nanocarrier based on bovine serum albumin (BSA) and reduced grapheme oxide (rGO) as a

novel vehicle for sustained release of carboplatin as an anticancer therapeutic agent. For this purpose, FTIR, SEM, DLS and zeta potential analyses were performed to discover the nature of the nanocarrier and its function on anticancer drug release with different ratios of rGO and BSANP (1:1, 1:5 and 1:10). FTIR results confirmed the presence of BSANP and rGO in nanocarrier. Further, the SEM analysis indicated that BSANP coated rGO sheets, and it has a spherical shape with dimensions below 200 nm. Moreover, the drug loading and entrapment efficacy were determined, and the drug release behavior of rGO, BSANP, rGO-BSANP (1:1, 1:5, 1:10) was investigated using absorption spectroscopy. The rGO-BSANP (1:1) system was shown to be an appropriate drug carrier due to a 100% release at 300 min. The release mechanism was studied, indicating that all of the carriers followed non-Fickian diffusion. The cytotoxicity was evaluated on human breast cancer cell lines, MCF-7, showing the decrease of IC_{50} value of carboplatin in the presence of nanocarrier. Altogether, the designed system could be a promising carrier for the effective treatment of breast cancer cells.

ACKNOWLEDGMENTS

This research work has been supported with research grant (No. 771395067) by Materials and Energy Research Center (MERC), Karaj, Iran.

REFERENCES

[1] J. Folkman, D.M. Long, J. Surg. Res. 4 (1964) 139.
[2] N.Y. Abu-Thabit, A.S.H. Makhlouf, Woodhead Publishing 1 (2018) 3.
[3] Z. Yu, M. Yu, Z. Zhang, G. Hong, Q. Xiong, Nanoscale Res. Lett. 9 (2014) 343.
[4] C.B. Dornelas, A.M. Silva, C.B. Dantas, C.R. Rodrigues, S.S. Coutinho, P.C. Sathler, H.C. Castro, L.R.S. Dias, V.P. Sousa, L.M. Cabral, J. Pharm. Pharm. Sci. 14 (2011) 17.
[5] S.K. Das, Am. J. Pharm. Edu. 70 (2006) 94.
[6] S.L. Harilall, Y.E. Choonara, G. Modi, L.K. Tomar, C. Tyagi, P. Kumar, L.C. du Toit, S.E. Iyuke, M. Danckwerts, V. Pillay, J. Pharm. Pharm. Sci. 16 (2013) 470.
[7] D. Wang, S.J. Lippard, Nat. Rev. Drug Discov. 4 (2005) 307.
[8] T. Sadhukha, S. Prabha, AAPS Pharm. Sci. Tech. 15 (2014) 1029.
[9] D. Liu, C. He, A.Z. Wang, W. Lin, Int. J Nanomed. 8 (2013) 3309.
[10] K. Greish, Methods Mol. Biol. 624 (2010) 25.
[11] M. Shi, M. Anantha, M. Wehbe, M.B. Bally, D. Fortin, L.-O. Roy, G. Charest, M. Richer, B. Paquette, L. Sanche, J. Nanobiotech. 16 (2018) 77.
[12] B. Ghalandari, A. Divsalar, A. Komeili, M. Eslami-Moghadam, A.A. Saboury, K. Parivar, Biomacromol. J. 1 (2015) 204.
[13] A.M.M.T. Mehmood, A.B. Iyer, S. Arif, M. Junaid, R.S. Khan, W. Nazir, N. Khalid, Woodhead Publishing (2019) 161.
[14] A.O. Elzoghby, W.M. Samy, N.A. Elgindy, J. Control Release 157 (2012) 168.
[15] R. Lima-Sousa, D. de Melo-Diogo, C.G. Alves, E.C. Costa, P. Ferreira, I.J. Louro, Carbohyd Pol 200 (2018) 93.
[16] Z. Sheng, L. Song, J. Zheng, D. Hu, M. He, M. Zheng, G. Gao, P. Gong, P. Zhang, Y. Ma, L. Cai, Biomat 34 (2013) 5236.
[17] W. Wang, Y. Huang, S. Zhao, T. Shao, Y. Cheng, Chem. Commun. 49 (2013) 2234.
[18] K. Langer, S. Balthasar, V. Vogel, N. Dinauer, H. von Briesen, D. Schubert, Int. J. Pharm. 2003, 257(1-2): 169-180.
[19] C. Weber, J. Kreuter, K. Langer, Int. J. Pharm. 196 (2000) 197.
[20] K. Langer, M.G. Anhorn, I. Steinhauser, S. Dreis, D. Celebi, N. Schrickel, S. Faust, V. Vogel, Int. J. Pharm. 347 (2008) 109.
[21] K. Westesen, H. Bunjes, M.H.J. Koch, J. Control. Release 48 (1997) 223.
[22] S. D'Souza, Adv. Pharm. 2014 (2014) 1.
[23] V.N. Babu, S. Kannan, Int. J. Biol. Macromol. 51 (2012) 1103.
[24] G.-H. Son, B.-J. Lee, C.-W. Cho, J. Pharm. Inv. 47 (2017) 287.
[25] P. Zhang, T.-Y. Wang, H.-M. Xiong, J.-L. Kong, Talanta 127 (2014) 43.
[26] Ö.S. Aslantürk, *In Vitro* Cytotoxicity and Cell

Viability Assays: Principles, Advantages, and Disadvantages. Vol. 2, 2018: InTech.
[27] J. Grdadolnik, Y. Marechal, Biopol. 62 (2001) 54.
[28] J. Grdadolnik, Y. Marechal, Biopol. 62 (2001) 40.
[29] C. Xu, X. Shi, A. Ji, L. Shi, C. Zhou, Y. Cui, PloS one 10 (2015) e0144842.
[30] S. Rohiwal, A. Tiwari, G. Verma, S. Pawar, Colloid Surf. A 480 (2015) 28.
[31] Y. Fu, W.J. Kao, Expert. Opin. Drug Deliv. 7 (2010) 429.
[32] S. Gurunathan, J.W. Han, V. Eppakayala, J.H. Kim, Int. J. Nanomedicine 8 (2013) 1015.